# Decay of the $I^\pi = 8^-$ isomeric state in $^{134}$Nd and $^{184}$Pt studied by electron and $\gamma$ spectroscopy

J. Perkowski* and J. Andrzejewski
*Faculty of Physics and Applied Informatics, University of Łódź, 90-236 Łódź, Poland*

Ch. Droste, Ł. Janiak, E. Grodner, and S. G. Rohoziński
*Faculty of Physics, University of Warsaw, 02-093 Warsaw, Poland*

L. Próchniak, J. Srebrny, J. Samorajczyk-Pyśk, T. Abraham, K. Hadyńska-Klęk, M. Kisieliński, M. Komorowska, M. Kowalczyk, J. Kownacki, T. Marchlewski, J. Mierzejewski, P. Napiorkowski, and A. Stolarz
*Heavy Ion Laboratory, University of Warsaw, 02-093 Warsaw, Poland*

A. Korman
*National Centre for Nuclear Research, 05-400 Otwock, Świerk, Poland*

M. Zielińska
*Irfu, CEA, Université Paris-Saclay, F-91191 Gif-sur-Yvette, France*
(Received 7 June 2016; revised manuscript received 25 October 2016; published 5 January 2017)

The properties of the $K$-isomer decays in the $^{134}$Nd and $^{184}$Pt nuclei have been investigated. Measurements were carried out in $e$-$\gamma$ and $\gamma$-$\gamma$ coincidence modes using electron spectrometers coupled to the central European Array for Gamma Levels Evaluations at the Heavy Ion Laboratory of the University of Warsaw. Internal conversion coefficients were obtained for transitions relevant to the decay of the isomeric states, allowing the determination of multipolarities and mixing ratios as well as hindrance factors. Two possible causes of the weakening of the $K$ forbiddenness, namely rotational $K$ mixing (Coriolis interaction) and triaxiality, are briefly discussed using schematic theoretical models.

DOI: 10.1103/PhysRevC.95.014305

## I. INTRODUCTION

Nuclear isomerism is a frequently observed phenomenon. According to a recent compilation [1], there are 2469 isomers with half-life $T_{1/2} \geqslant 10$ ns. They are classified into five groups [1], including the group of $K$ isomers. The mechanism of electromagnetic decay of these isomers, in spite of being the subject of extensive studies, is still frequently discussed [2–8]. $K$-isomeric states with spin/parity $I^\pi = 8^-$ and quantum number $K$ equal to 8 (where $K$ is the projection of the total angular momentum onto the symmetry axis of the nucleus) are found in nuclei from the mass regions around $A = 130$, 180, and 250. These isomeric states are observed in even-even nuclei with neutron numbers $N = 74$, 106, and 150 and in some isotopes of hafnium ($Z = 72$) and tungsten ($Z = 74$). They often decay many orders of magnitude slower than expected from the Weisskopf single-particle estimate. As an example, the $I^\pi = 8^-$, $K = 8$, 2340 keV, $T_{1/2} = 9.4$ ms isomeric state in $^{132}_{58}Ce_{74}$ [9] decays, among other ways, to the $6^+$ state (a member of the ground-state band with $K = 0$) via mixed $E3/M2$ transitions. For this decay the hindrance factors defined as $F = T^p_{1/2}/T^W_{1/2}$ (where $T^p_{1/2}$ is the partial half-life of the isomeric state and $T^W_{1/2}$ is the corresponding Weisskopf estimate) are equal to $2.5(4)\times10^3$ and $4(1)\times10^6$ for the $E3$ and $M2$ transitions [9], respectively.

Within the model of axially symmetric deformed (prolate) nuclei the isomeric $I^\pi = 8^-$, $K = 8$ states in $^{134}$Nd and $^{184}$Pt can be described by the following two quasiparticle configurations: $\nu 7/2[404] \otimes \nu 9/2[514]$ ($N = 74$) and $\nu 7/2[514] \otimes \nu 9/2[624]$ ($N = 106$) [1], with a single value of $K = 8$. These isomeric states decay via $E1$ transitions to the $I^\pi = 8^+$ state belonging to the ground-state band. For an axially symmetric nucleus this state has a value of $K$ equal to 0. Such $E1$ transitions have been found in, among others, $^{134}$Nd ($N = 74$) and $^{184}$Pt ($N = 106$) [10–14]. Additionally, $E3/M2$ or $E3$ transitions are observed in nuclei with neutron number $N = 74$, where they connect the isomeric state with the $I^\pi = 6^+$ state [9–15] of the rotational band with $K = 0$ as well as with the $I^\pi = 5^+$ state [9–15] belonging to the $\gamma$ band with $K = 2$. According to the selection rules, $2^\lambda$-pole transitions between initial ($i$) and final ($f$) states with quantum numbers $K_i$ and $K_f$, respectively, are allowed if the condition $\Delta K = |K_i - K_f| \leqslant \lambda$ is fulfilled. Therefore, in an axially symmetric deformed nucleus where the $K$ quantum number is a good one, the above-mentioned transitions ($E1, M2, E3$) between states with $K_i = 8$ and $K_f = 0$ or 2 should be forbidden. In fact, however, they are observed as strongly slowed down but not truly forbidden. This suggests that in these cases $K$ is not a good quantum number and that the isomeric states and/or the final states have (in addition to the main value of $K$) some admixtures of other $K$ components. The presence of these admixtures enables the decay of the $K$-isomeric state. One possible reason for the $K$ admixtures is the Coriolis interaction that can modify the wave function

*jarekper@uni.lodz.pl

 

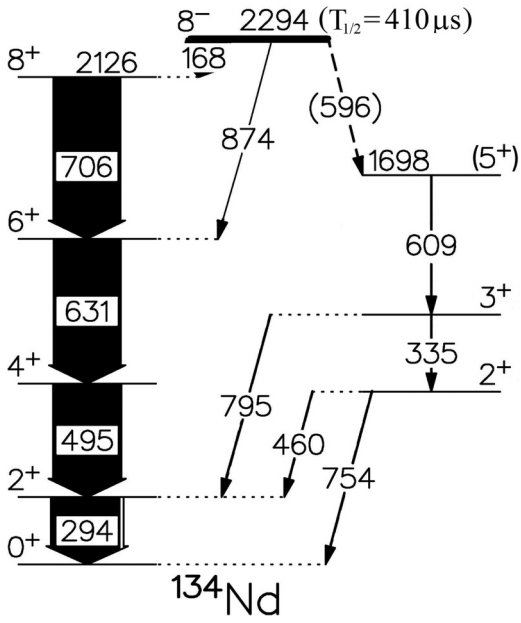


FIG. 1. The decay scheme of the $I^{\pi} = 8^{-}$, $K = 8$ isomeric state in $^{134}$Nd ($N = 74$) [10,11].

of the states to which an isomer decays, adding to the main value of $K$ some additional high-$K$ components [2–4]. There is another possible source of such admixtures, namely a deviation of the nuclear shape from axial symmetry. In such a case the nuclear-state wave functions are obviously combinations of components with different $K$ values. To evaluate quantitatively the contribution of higher-$K$ components, we have applied the simple phenomenological Davydov-Filippov model [16] of a triaxial rigid rotor. The estimated value of the triaxiality parameter $\gamma$ [17] for the nuclei considered is around 20°–25° (see Sec. III), which causes the higher-$K$ contribution to be quite substantial. Hence, both mechanisms of the $K$ mixing should be taken into account for transitional nuclei such as $^{134}$Nd and $^{184}$Pt.

In this work both conversion electrons and $\gamma$ rays were studied, which allowed the internal conversion coefficients (ICCs) and, as a consequence, the multipolarities to be determined. This information can be further used for measuring absolute transition probabilities. The experiment and results are described in Sec. II. Theoretical considerations and a summary are given in Secs. III and IV, respectively.

## II. EXPERIMENTS

The half-lives of the studied $I^{\pi} = 8^{-}$, $K = 8$ isomeric states in the $^{134}$Nd and $^{184}$Pt nuclei are of the order of 1 ms; hence, the measurements were carried out during "beam-off" time intervals in electron-$\gamma$ and $\gamma$-$\gamma$ coincidence modes. The decay schemes of the $I^{\pi} = 8^{-}$, $K = 8$ isomeric states for the measured nuclei are presented in Fig. 1 for $^{134}$Nd [10,11] and Fig. 2 for $^{184}$Pt [13]. $E1$ ($8^{-} \rightarrow 8^{+}$) and $E3$ ($8^{-} \rightarrow 6^{+}$) transitions with a degree of $K$ forbiddenness $\nu = |K_i - K_f| - \lambda = 7$ and 5 leading directly to the $8^{+}$ and $6^{+}$ states of the ground-state band with $K = 0$ are present in $^{134}$Nd (see Table I). Also, in the $^{184}$Pt decay scheme an $E1$ transition connects the $I^{\pi} = 8^{-}$, $K = 8$ isomeric state with the $8^{+}$ state belonging to the ground-state rotational band ($K = 0$). All these $\gamma$ transitions severely violate the purity of the $K$-quantum number. Admixtures of $K$-quantum numbers are important for the description of configurations of excited states in both nuclei.

The decays of the isomeric states in $^{134}$Nd and $^{184}$Pt were studied using the EAGLE array [18] and conversion-electron spectrometers. The EAGLE array (central European Array for Gamma Levels Evaluations), located at the Heavy Ion Laboratory of University of Warsaw, has been designed as a multidetector setup for in-beam nuclear spectroscopy studies. In our experiments the array was equipped with 15

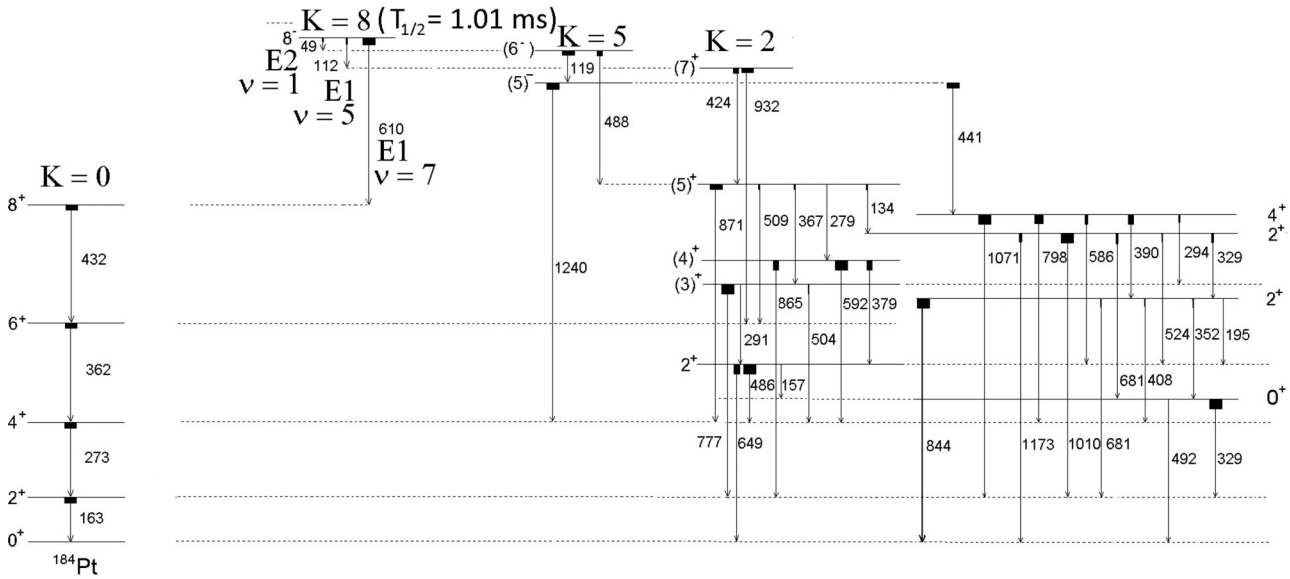


FIG. 2. The decay scheme of the $I^{\pi} = 8^{-}$ isomeric state in $^{184}$Pt ($N = 106$) [13]. The width of the solid rectangles at the top of the arrows is proportional to the relative $\gamma$ intensity from a given level.

TABLE I. Summary of data for the $8^-$ isomeric state in $^{134}$Nd. The table contains information about energies ($E_\gamma$), intensities ($I_\gamma$), spins ($I_i$, $I_f$), multipolarities ($\sigma\lambda$), partial half-lives ($T^p_{1/2}$), reduced transition probabilities [$B(\sigma\lambda, i \to f)$], hindrance factors ($F$), degree of $K$ forbiddenness ($\nu$), and reduced hindrance factors $f_\nu = F^{1/\nu}$ in the convention used in our work and in Ref. [8] (see the penultimate and the last column, respectively).

| $E_\gamma$ (keV) | $I_\gamma$[a] | $I_i$[a] | $I_f$[a] | $\sigma\lambda$ | $T^p_{1/2}$ (ms) | $B(\sigma\lambda, i \to f)$ | $F$[b] | $\nu$ | $f_\nu$[b] | $f_\nu$[c] |
|---|---|---|---|---|---|---|---|---|---|---|
| 168 | 93(7) | $8^-$ | $8^+$ | $E1$ | 0.47(5) | $2.0(2)\times10^{-10}$ ($e^2$ fm$^2$) | $8.4(9)\times10^5$ | 7 | $7.0^{+0.1}_{-0.1}$ | $26.2^{+0.4}_{-0.4}$ |
| 596 | 0.6(2) | $8^-$ | $(5^+)$ | $E3$[d] | 73(25) | $0.6^{+0.3}_{-0.16}$ ($e^2$ fm$^6$) | $1.7(6)\times10^3$ | 3 | $11.9^{+1.2}_{-1.6}$ | $11.9^{+1.2}_{-1.6}$ |
| 874 | 7(2) | $8^-$ | $6^+$ | $E3$[e] | $7^{+10}_{-3}$ | $0.5^{+0.4}_{-0.3}$ ($e^2$ fm$^6$) | $2^{+3}_{-1}\times10^3$ | 5 | $5^{+0.9}_{-0.5}$ | $5^{+0.9}_{-0.5}$ |

[a]Intensities $I_\gamma$ of the 168- and 874-keV $\gamma$ transitions and all spin values ($I_i$, $I_f$) were taken from Ref. [11].
[b]Convention used in this work; see text.
[c]Convention used in Ref. [8].
[d]Spin/parity $I^\pi_f = 5^+$ was assumed.
[e]Only pure $E3$ multipolarity is considered; however, in the limit of experimental uncertainty an $M2$ admixture is possible (see text in Sec. II).

Compton-suppressed Ge detectors and was coupled to a conversion-electron spectrometer. The conversion-electron spectrometer used in the $^{134}$Nd experiment was constructed at the University of Łódź [19] for "in-beam" studies. The spectrometer utilizes a combination of two magnetic fields for separation and transportation of electrons from the target position to the silicon detectors. Separation of electrons from positrons is achieved in a simplified miniorange setup. The transportation field is produced by a set of permanent magnets arranged in the form of coaxial rings. The background from $\delta$ electrons and $\gamma$ rays is greatly reduced. A new version of the spectrometer University of Lodz an Electron SpEctrometer (ULESE) [20] was used in the $^{184}$Pt experiment. The ULESE spectrometer is characterized by a very high efficiency, up to 9% at an energy of 300 keV, and good energy resolution, $\approx$1% at $\sim$500 keV for a thin calibration source and, which is very important, good suppression of $\delta$ electrons, positrons, and photons emitted by the targets. This achievement was obtained using a combination of magnetic fields in two different layouts: perpendicular and parallel to the axis of the spectrometer, which is orthogonal to the beam line. Both spectrometers were designed to be coupled to the EAGLE array.

Internal conversion coefficients $\alpha$ were determined based on the formula [9]

$$\alpha = \frac{N_e}{N_\gamma}\frac{\epsilon_\gamma}{\epsilon_e}, \tag{1}$$

where $N_e$ and $N_\gamma$ are the numbers of conversion electrons and $\gamma$'s for a given transition, $\epsilon_e$ and $\epsilon_\gamma$ are the detection efficiencies of the electron and $\gamma$ spectrometers, respectively.

The efficiency curve ($\epsilon_\gamma/\epsilon_e$) as a function of electron energy was obtained based on transitions with well-known multipolarity or known ICC. The GF3 program from the RADWARE package [21] was used to analyze the $\gamma$ and electron lines. For the fitting procedure of electron peaks a step function and an asymmetric Gaussian were used in addition to the usual Gaussian shape.

### A. Decay of the $I^\pi = 8^-$, $K = 8$ isomeric state in $^{134}_{60}$Nd$_{74}$

The $^{134}$Nd nucleus was produced in the $^{122}$Te($^{16}$O,4$n$)$^{134}$Nd reaction at a beam energy of 90 MeV and an intensity of about 10 pnA. The $^{16}$O beam was delivered by the U-200P cyclotron of the Heavy Ion Laboratory (HIL) of the University of Warsaw. The $^{122}$Te target (with thickness of about 3 mg/cm$^2$) was evaporated onto a Au backing foil (2.5 mg/cm$^2$) thick enough to stop all recoils. The target preparation is described in Ref. [22].

The efficiency curve (Fig. 3) of our setup was obtained using an internal calibration based on the $\gamma$ transitions accompanying the $^{134m}$Nd $\to$ $^{134}$Nd and $^{134}$Nd $\to$ $^{134}$Pr $\to$ $^{134}$Ce decays. The following lines with well-known multipolarities were used: 495, 631, and 706 keV from $^{134}$Nd and 409, 556, 639, 677, 965, and 973 keV from the $^{134}$Pr $\to$ $^{134}$Ce decay.

One of the main goals of this experiment was to determine the internal conversion coefficient for the 874-keV transition which connects the isomeric state with the $6^+$ level in the $^{134}$Nd nucleus (Fig. 1). To clean up the $\gamma$ and electron spectra from long-lived ($T_{1/2} \geqslant 1$ ms) lines which do not originate from the isomeric state decay ($T_{1/2} \approx 0.4$ ms), events collected between 2.1 and 3.6 ms after the end of the cyclotron beam pulse were subtracted from the events collected in the time span between 0.2 and 1.7 ms. This method could be used owing to the millisecond time structure of the cyclotron beam at the HIL ("beam-on," 2 ms; "beam-off," 4 ms). The electron spectrum (the sum of three spectra gated on the 294-, 495-, and 631-keV

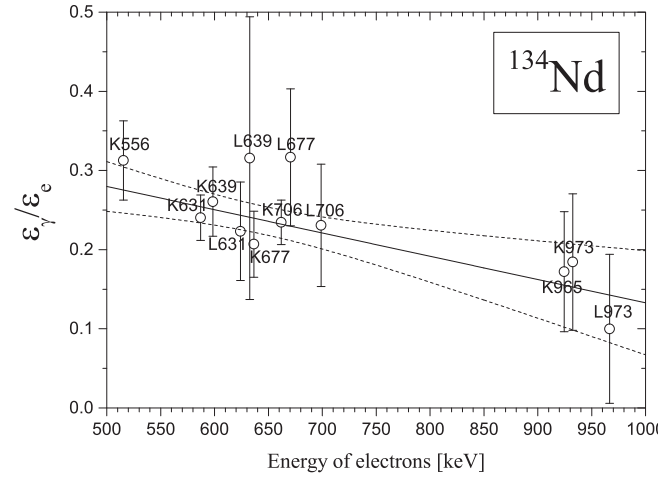


FIG. 3. The efficiency curve ($\epsilon_\gamma/\epsilon_e$) of the experimental setup for the $^{134}$Nd measurement. The linear fit to the experimental points and the error band are indicated by solid and dashed lines, respectively.

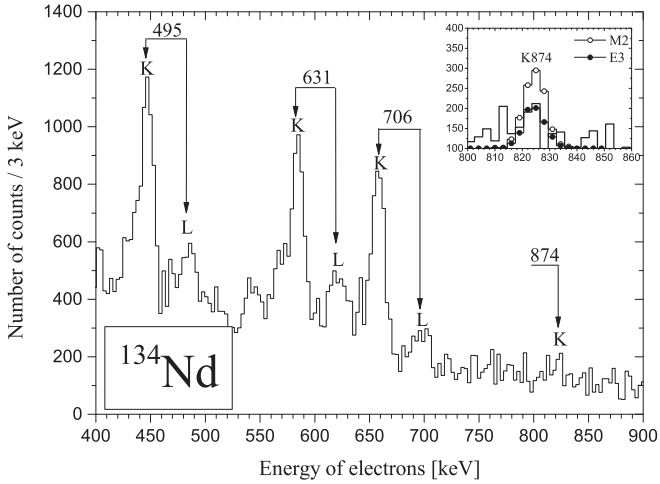


FIG. 4. The summed electron spectrum in coincidence with the 294-, 495-, and 631-keV $\gamma$ transitions accompanying the decay of the isomeric state in $^{134}$Nd (see also Fig. 1). The experimental (thick solid line) and simulated (for more details, see text) K874 lines, for $M2$ and $E3$ multipolarities, are shown for comparison in the inset.

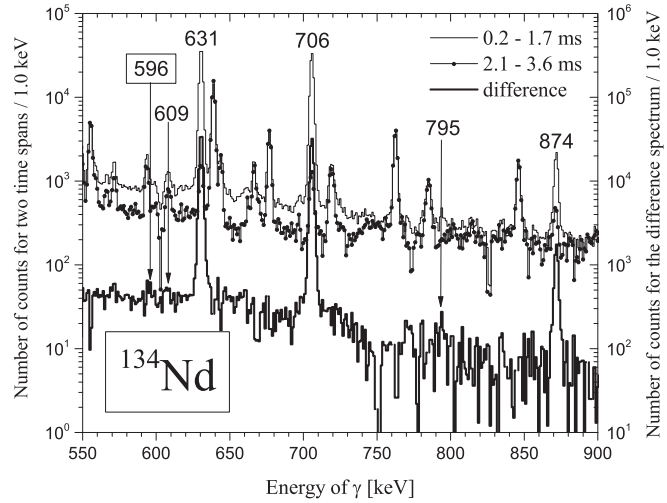


FIG. 5. The $\gamma$ spectra (thin solid lines, left ordinate) gated on the 294-keV line collected during two time spans (see text) after the end of the cyclotron beam pulse. The weak 596-keV $\gamma$ line is visible in the difference spectrum (thick solid line, right ordinate). This proves that the $8^-$ isomeric state in $^{134}$Nd also decays to the $\gamma$ band, as was suggested in Ref. [10].

$\gamma$ lines) is presented in Fig. 4. By analyzing this spectrum, the value of the conversion coefficient for the $8^- \rightarrow 6^+$, K874 line was determined to be $\alpha_K = 0.005(2)$. Comparison of this value with theoretical conversion coefficients ($\alpha_K(E3) = 0.005\,51$, $\alpha_K(M2) = 0.0103$ [23]) suggests that the studied transition has a pure $E3$ or mixed $E3/M2$ character in the limit of experimental uncertainty. It is worth adding that previously available information suggesting an $M2$ multipolarity for the 874-keV transition [12] was based purely on systematics. For a better visualization of our result, the inset in Fig. 4 shows the part of the electron spectrum relevant to the K874 line. The experimental spectrum can be compared with the simulated electron peaks for $M2$ and $E3$ multipolarities. The simulated electron spectra were calculated taking into account the experimentally obtained intensity of the $\gamma$'s, the efficiency of the experimental setup and the experimental energy resolution of the electron spectrometer.

The possibility that the $8^-$ isomeric state decays to the $(5^+)$ level via the 596-keV transition (see Fig. 1) was pointed out in Ref. [10]. To check this suggestion, the $\gamma$-ray spectrum gated on the 294-keV line was analyzed (see Fig. 5). Thanks to the time-cleaning procedure (described above) a very weak 596-keV $\gamma$ line was observed (Fig. 5), showing that this isomer decays to the $(5^+)$, 1698-keV level belonging to the $\gamma$ band and then via the 609- and 795-keV transitions to the $2^+$ state of the rotational band. The decay path of the $(5^+)$ level via emission of the 609-, 795-, and 294-keV $\gamma$'s is well established [10–12]. Our observation supports the result that the 596-, 609-, and 795-keV transitions are not present in the $\gamma$ spectrum gated on the 495-keV line. The intensity of the 596-keV line was estimated at 0.6(2)%. For comparison, the $\gamma$ intensities of the 168- and 874-keV transitions connecting the $8^-$ state with the $8^+$ and $6^+$ states are 93% and 6.5%, respectively [12]. In this experiment the half-life of the $I^\pi = 8^-$, $K = 8$ isomeric state in $^{134}$Nd was measured as 0.38(2) ms and this value agrees perfectly with the value of 0.41(3) ms given in Ref. [12].

### B. Decay of the $I^\pi = 8^-$, $K = 8$ isomeric state in $^{184}_{78}Pt_{106}$

The study of the decay of the $I^\pi = 8^-$, $K = 8$ isomeric state in $^{184}$Pt was performed by measuring $e$-$\gamma$ and $\gamma$-$\gamma$ coincidences. The $^{184}$Pt isotope was produced in the $^{175}$Lu($^{14}$N,5$n$)$^{184}$Pt reaction at a beam energy of 90 MeV and intensity of about 1 pnA. The $^{14}$N beam was delivered by the U-200P cyclotron of the Heavy Ion Laboratory, Warsaw. In the experiment natural lutetium foil (2.5 mg/cm$^2$ thick) was used as a target. The Lu foil was backed by a gold layer ($\sim$1 mg/cm$^2$) to stop all the reaction products. Therefore, electrons as well as $\gamma$ rays were emitted from a well-defined spot. The chosen thickness of the target was a compromise between the energy loss of electrons traveling through the target and the efficiency of $^{184}$Pt production.

In this experiment the EAGLE array and the ULESE conversion-electron spectrometer were used. As an example of the data obtained from this electron spectrometer, spectra of electrons emitted from the target during "beam-off" periods are shown in Fig. 6.

In this experiment the efficiency curve (see Fig. 7) was obtained using an internal calibration based on the $\gamma$ transitions accompanying the $^{184m}$Pt $\rightarrow$ $^{184}$Pt and $^{184}$Pt $\rightarrow$ $^{184}$Ir $\rightarrow$ $^{184}$Os decays. The following lines with well-known multipolarities were used: 163, 273, 362, 432, and 610 keV from $^{184}$Pt and 120, 264, 390, 493, and 539 keV from the $^{184}$Ir $\rightarrow$ $^{184}$Os decay. A third-order polynomial function was fitted to the experimental points. The result is shown in Fig. 7.

One of the goals of the $^{184}$Pt experiment was the determination of the conversion coefficient for the $(6^-) \rightarrow (5)^-$, 119-keV transition (see Fig. 2). For that purpose the electron spectra in coincidence with the 441- and 1071-keV $\gamma$ rays were summed. The resulting spectrum is shown in Fig. 8 as the thin solid line. A conversion coefficient for the $L + M + \cdots$ lines equal to $\alpha_{L+M+\cdots} = 1.2(2)$ was obtained. This value agrees with

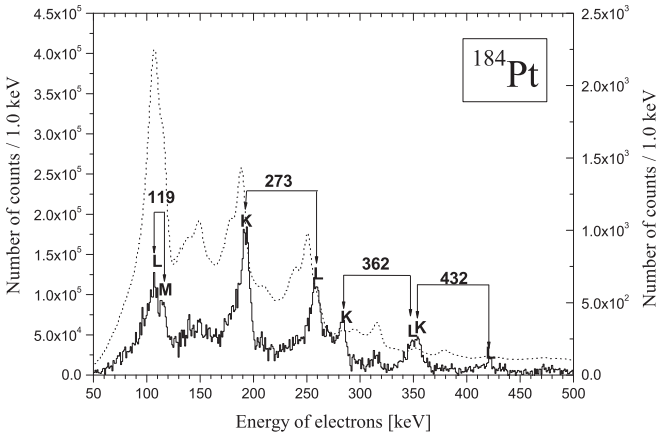


FIG. 6. The total electron spectrum (dotted line, left ordinate) and the spectrum gated on the 163-keV $\gamma$ line (solid line, right ordinate) for the $^{184}$Pt "beam-off" measurement.

$\alpha_{L+M+...}(E2) = 1.5(3)$ published in Ref. [14]. A comparison of our result with theoretical conversion coefficients for the 119-keV transition ($\alpha_{L+M+...}(E1) = 0.05$, $\alpha_{L+M+...}(E2) = 1.87$, $\alpha_{L+M+...}(M1) = 0.72$, $\alpha_{L+M+...}(M2) = 9.4$ [23]) implies an $E2/M1$ mixed transition with $\delta^2 = 0.7^{+0.9}_{-0.4}$. The $E2/M1$ transition is consistent with the level scheme (Fig. 2) proposed in Ref. [13]. An $M2/E1$ solution with a substantial contribution from the $M2$ transition (our result $\delta^2 = 0.14(3)$ and the result from Ref. [14] $\delta^2 = 0.19$) is also possible.

Another important transition in the decay of the $I^{\pi} = 8^{-}$, $K = 8$ isomeric state in $^{184}$Pt is the $(6^{-}) \rightarrow (5)^{+}$, 488-keV line. From the electron spectrum presented in Fig. 9 it was only possible to obtain an upper limit for the internal conversion coefficient of the studied transition: $\alpha_K \leqslant 0.028(2\sigma)$. By comparing this result with the calculated ICCs ($\alpha_K(E1) = 0.0073$, $\alpha_K(M1) = 0.069$, $\alpha_K(E2) = 0.019$ and $\alpha_K(M2) = 0.20$ [23]) one can draw the conclusion that the following solutions,

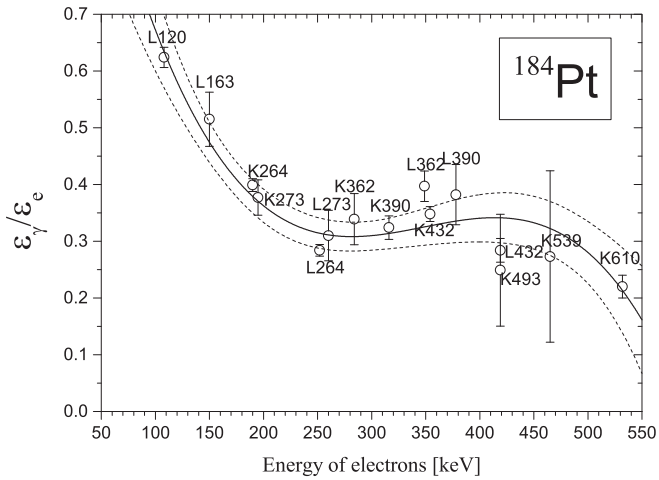


FIG. 7. The efficiency curve ($\epsilon_\gamma/\epsilon_e$) vs electron energy for the experimental setup ($^{184}$Pt experiment). The third-order polynomial fit to the experimental points and the error band are denoted by solid and dashed lines, respectively.

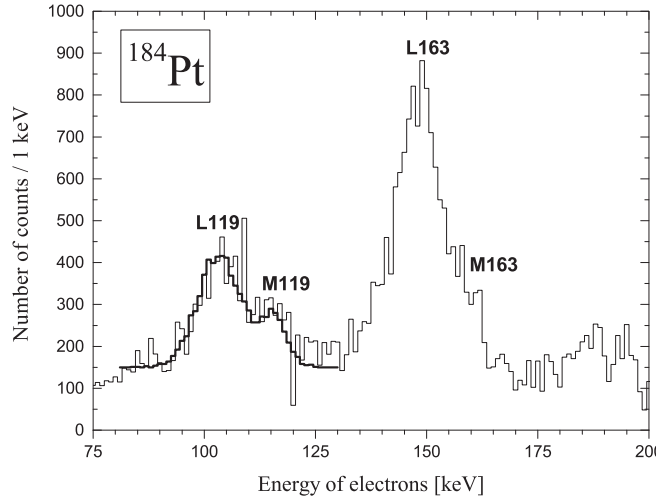


FIG. 8. Sum of the electron spectra (thin solid line) in coincidence with the 441- and 1071-keV $\gamma$ rays from the $^{184}$Pt experiment. For the 119-keV transition the experimental spectrum may be compared with the simulated one (thick solid line) for $\delta^2 = 0.7$.

namely $E1$ (or $E1/M2$) and $E2$ (or $E2/M1$), should be considered. The $E1$ or $E1/M2$ multipolarities agree with the assignment of spins/parities proposed in Ref. [13] for the $(6^{-}) \rightarrow (5)^{+}$ transition, whereas the $E2$ (or $E2/M1$) multipolarity requires $\Delta I = |I_{\text{initial}} - I_{\text{final}}| = 2$ or 1 and $\Delta\pi = \pi_{\text{initial}} \times \pi_{\text{final}} = +1$ for the spins/parities of the studied transition.

In the case of the $(7)^{+} \rightarrow (5)^{+}$, K424-keV line the situation is more complicated. One broad electron peak at an energy of 350 keV in the sum of the electron spectra gated by the 163-, 273-, and 871-keV transitions consists of the K432-keV ($E_e = 354$ keV), L362-keV ($E_e = 349$ keV), and K424-keV ($E_e = 346$ keV) lines. Fortunately, the multipolarities of the 362- and 432-keV transitions are known from Ref. [13]

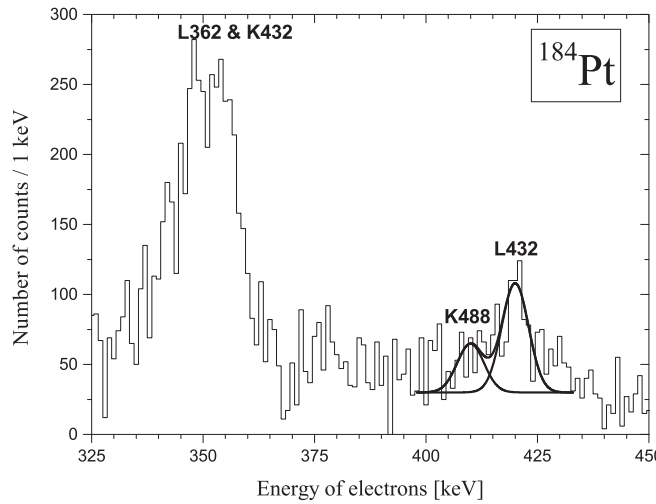


FIG. 9. The sum of the electron spectra gated on the 163- and 871-keV $\gamma$ lines from $^{184}$Pt. The thick solid line represents a Gaussian function (superimposed on a constant background) fitted to the experimental points. All peak parameters were fixed except the area.

TABLE II. The same as Table I but for the $8^-$ isomeric state in $^{184}$Pt.

| $E_\gamma$ (keV) | $I_\gamma$[a] | $I_i$ | $I_f$ | $\sigma\lambda$ | $T^p_{1/2}$ (ms) | $B(\sigma\lambda, i \to f)$ | $F$[b] | $\nu$ | $f_\nu$[b] | $f_\nu$[c] |
|---|---|---|---|---|---|---|---|---|---|---|
| 49 | 0.79(8) | $8^-$ | $(6^-)$ | $E2$[d] | 300(40) | $6.7(9)\times10^{-3}$ ($e^2$ fm$^4$) | $9(1)\times10^3$ | 1 | $9^{+1}_{-1}\times10^3$ | $9^{+1}_{-1}\times10^3$ |
| 112 | 12(4) | $8^-$ | $(7)^+$ | $E1$ | 19(7) | $1.6^{+0.9}_{-0.4}\times10^{-11}$ ($e^2$ fm$^2$) | $1.2(4)\times10^7$ | 5 | $26.2^{+1.6}_{-2.1}$ | $165^{+10}_{-13}$ |
| 610 | 100(16) | $8^-$ | $8^+$ | $E1$[d] | 2.3(4) | $8.0(1.5)\times10^{-13}$ ($e^2$ fm$^2$) | $2.6(5)\times10^8$ | 7 | $15.9^{+0.4}_{-0.5}$ | $59.2^{+1.4}_{-1.7}$ |

[a]Intensities of listed $\gamma$ transitions ($I_\gamma$) were taken from Ref. [13] except for the 49-keV line.
[b]Convention used in this work; see text.
[c]Convention used in Ref. [8].
[d]Multipolarity taken from Ref. [13].

and the $\gamma$ lines of these peaks are easily identified in the $\gamma$ spectrum; therefore, the ICC for the 424-keV transition could be calculated from the equation

$$\alpha_K^{424} = \frac{N_e^{424+362+432}(\epsilon_\gamma/\epsilon_e) - \alpha_K^{432}N_\gamma^{432} - \alpha_L^{362}N_\gamma^{362}}{N_\gamma^{424}} = -0.09 \pm 0.08, \quad (2)$$

where $\alpha_K$ and $\alpha_L$ are the internal conversion coefficients for the given transition, $N_e$ and $N_\gamma$ are the numbers of conversion electrons and $\gamma$'s for the transitions of interest, and $\epsilon_\gamma/\epsilon_e$ is the detection efficiency of the experimental setup.

In this equation the efficiency ratios were assumed to be the same for all transitions considered. As a result, it was only possible to obtain an upper limit for the ICCs of the studied transition: $\alpha_K \leqslant 0.07(2\sigma)$. A comparison of this result with the calculated ICCs ($\alpha_K(E1) = 0.0098, \alpha_K(M1) = 0.10$, $\alpha_K(E2) = 0.027$ and $\alpha_K(M2) = 0.31$ [23]) suggests that the studied $(7)^+ \to (5)^+$, 424-keV transition has $E2$ multipolarity (in agreement with Ref. [13]) or $E2/M1$. The $E1$ or $E1/M2$ multipolarities are excluded because of the parities of the initial and final states. There are no other data concerning the ICCs for the 424- and 488-keV transitions that can be compared with our results.

In our experiment the $\gamma$-ray intensity of the $8^- \to (6^-)$, 49-keV transition was determined to be $I_\gamma = 0.79(8)\%$, assuming that the intensity of the $8^- \to 8^+$, 610-keV $\gamma$ transition equals 100% (see Table II). This result was obtained based on a comparison of the 119- and 112-keV line intensities in the $\gamma$ spectrum with a gate set on the $(2^+ \to 0^+)$, 163-keV transition. The accepted values of the ICCs for the 49-, 119-, and 488-keV transitions were used in this calculation.

In this experiment the half-life of the $I^\pi = 8^-$, $K = 8$ isomeric state in $^{184}$Pt was measured to be 0.86(10) ms. This value agrees with the value of 1.01(5) ms given in Ref. [13].

The experimental results (present work and also results taken from Ref. [11]) for the $I^\pi = 8^-$, $K = 8$ isomeric state in $^{134}$Nd are summarized in Table I. The results for the $E1$ transitions in $^{134}$Nd as well as in $^{184}$Pt require some additional comments. In our work, for $E1$ transitions the Weisskopf estimates of $T^W_{1/2}$ (used to calculate the value of $F$) were multiplied by a factor of $10^4$ to take into account the generally higher hindrance for such transitions [5,24,25]. It should be noted that Kondev *et al.* in their recent comprehensive review [8] did not use this correction factor. Hence, $F(E1;$ Kondev, Ref. [8]$) = 10^4 \times F(E1;$ our work) and the reduced hindrance factor per degree of $K$ forbiddenness $f_\nu(E1;$ Kondev, Ref. [8]$) = (10^4)^{1/\nu} \times f_\nu(E1;$ our work); see Table I for the definition of $f_\nu$. To avoid misunderstanding, in the last and penultimate columns of Tables I ($^{134}$Nd) and II ($^{184}$Pt) the same sets of experimental data are presented using both our and Kondev's conventions. The experimentally determined values of the internal conversion coefficients (taken from the present work and from Ref. [14]) for the $I^\pi = 8^-$, $K = 8$ isomeric state in $^{184}$Pt are summarized in Table III.

## III. THEORETICAL CONSIDERATIONS

Below we briefly discuss the two mechanisms which can be invoked to explain a reduction in the hindrance of a $K$-isomer decay. The first is the influence of the Coriolis interaction on nuclear states with increasing rotational frequency [3,7]. The second is deviation of the nuclear shape from axial symmetry, which can induce substantial higher $K$-number admixtures to nuclear wave functions [5,26]. In both cases we use simple phenomenological models which can give, we hope, some

TABLE III. Internal conversion coefficients (ICCs), multipolarities ($\sigma\lambda$), and mixing parameters ($\delta^2$) for transitions accompanying the decay of the $I^\pi = 8^-$, $K = 8$ isomeric state in $^{184}$Pt. The ICCs measured in the present work (second column) may be compared with the data of Ref. [13] (last column).

| $E_\gamma$ (keV) | ICC | $\sigma\lambda$, $\delta^2$ | ICC from Ref. [14] |
|---|---|---|---|
| 119 | $\alpha_{L+M} = 1.2(2)$ | $E2/M1$,[a] $\delta^2 = 0.7^{+0.9}_{-0.4}$ or $M2/E1$, $\delta^2 = 0.14(3)$ | $\alpha_{L+M} = 1.5(3)$ |
| 424 | $\alpha_K \leqslant 0.07(2\sigma)$ | $E2$ or $E2/M1$[b] | No data |
| 488 | $\alpha_K \leqslant 0.028(2\sigma)$ | $E1$ or $M2/E1$,[c] $E2$ or $E2/M1$[c] | No data |

[a]Multipolarity $E2/M1$ agrees with the $(6^-) \to (5)^-$ assignment given in Ref. [13].
[b]Multipolarity $E2$ agrees with the $(7)^+ \to (5)^+$ assignment given in Ref. [13].
[c]Multipolarities $E1$ or $E1/M2$ agree with the $(6^-) \to (5)^+$ assignment given in Ref. [13].

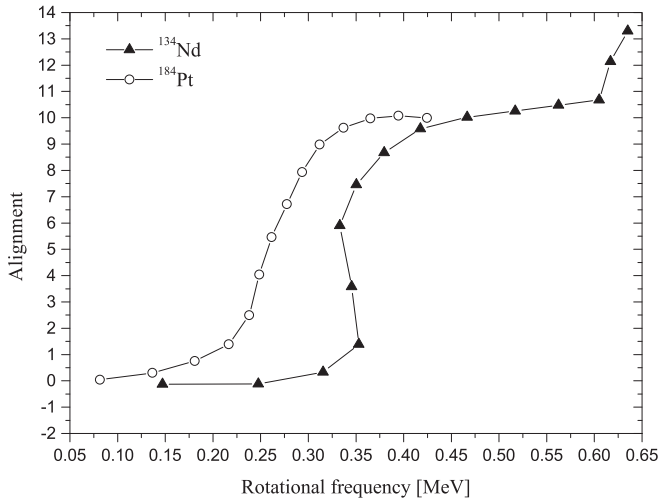


FIG. 10. Experimental alignments for $^{134}$Nd and $^{184}$Pt. Harris reference parameters of $\mathcal{I}_0 = 17.0\hbar^2$ MeV$^{-1}$ and $\mathcal{I}_1 = 25.0\hbar^2$ MeV$^{-1}$ (the same as in Ref. [3]) were used for both nuclei.

hints on the nature and decay of the $K$ isomers discussed even if the employed approximations are rather crude.

A high rotational frequency leads to changes of in the nuclear shell structure [27], and at some point the Coriolis force can break a correlated nucleon pair, which causes the creation of the so-called $s$ band. This effect can be seen, e.g., on a plot of the experimental alignments vs rotational frequency (Fig. 10). Other broken-pair excitations may have a substantial spin component along the symmetry axis, and as a result $K$-isomeric states emerge. However, the Coriolis effect can perturb the states to which an isomer decays and introduce higher-$K$ components into the wave function describing these states. These admixtures play the main role in the weakening of the hindrance of transitions from the $K$-isomeric state [3,8].

We performed band-mixing-type calculations according to the method described in Ref. [3]. In the first step the ground-state and $s$-band energies were parametrized using the well-known formula from the variable-moment-of-inertia (VMI) model [28],

$$E(I) = \frac{I(I+1)}{2J} + \frac{[(I(I+1)]^2}{8CJ^4} + E_0, \qquad (3)$$

where $I$ is the spin of a given level, $C$ and $E_0$ are constants, and the moment of inertia (depending on the spin) fulfills the equation

$$J^3 - J_0 J^2 + I(I+1)/2C = 0, \qquad (4)$$

with another constant $J_0$. The results of fitting the VMI parameters to experimental data and values of interaction matrix elements are given in Table IV. The calculations for $s$ bands were performed taking the value of the alignment as equal to $10\hbar$ for both nuclei (see Fig. 10). Final results for the distribution of $K$ values (after mixing the ground-state band and the $s$ band) are given in Table V. Let us mention that in the case of $^{134}$Nd a similar approach was used in Ref. [3] but with a different value for the alignment of the $s$ band ($6\hbar$).

The occurrence of higher-$K$ components in the final states of the decay of $K$ isomers in the considered nuclei as a consequence of nonaxial deformation (triaxiality) is studied using the simple phenomenological Davydov-Filippov model [16], which describes the energy of excited rotational states and electromagnetic transition probabilities for nonaxial nuclei. An important parameter of the model is the value of the $\gamma$ deformation which can be estimated, e.g., from the ratio of the excitation energies of the $2_1^+$ (yrast band) and of the $2_2^+$ level. From the experimental data we obtained values for the $\gamma$ deformation equal to 24° for $^{134}$Nd and 20° for $^{184}$Pt. An additional argument for considering the nonaxiality of the nuclei under study comes from our microscopic self-consistent calculations using the Sly4 Skyrme interaction and the $\delta$-type pairing. The calculations were made along the same lines as in Refs. [29,30]. The collective potential energy obtained for both nuclei is plotted in Fig. 11. One can observe a significant softness against nonaxial deformation, especially in the case of the $^{134}$Nd nucleus. In both cases the minimum of the collective energy corresponds to a nonzero $\gamma$ deformation.

The elaborate theoretical model used in Refs. [29,30], based on the generalized Bohr Hamiltonian, can also give more detailed information on collective states. One of the results obtained is the average value of the $\gamma$ deformation in the ground state, equal to 22° in the case of $^{134}$Nd and 18° in the case of $^{184}$Pt. These values are quite close to those calculated in the Davydov-Filippov (DF) model and we confine ourselves to the simpler DF approach because of several rather crude approximations employed in the subsequent discussion.

The following discussion is based mainly on the analysis of the distribution of wave-function components with different $K$ numbers of the $5^+$, $6^+$, $8^+$ (in $^{134}$Nd), $7^+$, $8^+$ (in $^{184}$Pt), and $8^-$ (for both nuclei) states. The results for the positive-parity states obtained from the two theoretical approaches mentioned previously are presented in Table V. Calculations for the Davydov-Filippov model were performed using the DF code [31]. In the case of the $\gamma$-vibrational band, owing to the lack of sufficient experimental information, we cannot apply the approach based on band mixing; hence, for the $5^+$ ($^{134}$Nd) and

TABLE IV. Parameters of the VMI model [28] and results of band mixing calculations for the considered nuclei.

| | | $C$ ($10^6$ keV$^3\hbar^{-4}$) | $J_0$ ($10^{-3}$ keV$^{-1}\hbar^2$) | $E_0$ (keV) | $V$ (keV)[a] | $s$ band (%)[b] |
|---|---|---|---|---|---|---|
| $^{134}$Nd | ground-state band | 4.9 | 7.8 | 0 | 275 | 2.8 |
| | $s$ band | 14.5 | 13 | 3634 | | |
| $^{184}$Pt | ground-state band | 1.6 | 19.6 | 24 | 114 | 0.6 |
| | $s$ band | 5.5 | 25 | 2669 | | |

[a]Interaction matrix element.
[b]Probability of admixture of the $s$ band in the $8^+$ yrast state.

TABLE V. Distributions of the $K$-number values calculated within the models discussed in the text for the relevant states in $^{134}$Nd and $^{184}$Pt. Each entry corresponds to the square of the amplitude (expressed in %) of a component of the wave function with a given $K$.

| | $^{134}$Nd | | | | | $^{184}$Pt | | | Ref. [7] |
|---|---|---|---|---|---|---|---|---|---|
| | DF model | | | Coriolis | | DF model | | Coriolis | |
| $KI^{\pi}$ | $5^+$ | $6^+$ | $8^+$ | $6^+$ | $8^+$ | $7^+$ | $8^+$ | $8^+$ | $8^-$ |
| 0 | – | 61.3 | 52.4 | 99.14 | 97.7 | – | 65.5 | 99.5 | 0 |
| 1 | – | – | – | 0.335 | 0.893 | – | – | 0.187 | 0 |
| 2 | 96.5 | 37.5 | 44.1 | 0.251 | 0.669 | 96.4 | 33.6 | 0.140 | 0 |
| 3 | – | – | – | 0.154 | 0.412 | – | – | 0.086 | 0 |
| 4 | 3.5 | 1.2 | 3.4 | 0.077 | 0.206 | 3.6 | 0.9 | 0.043 | $6.3\times10^{-4}$ |
| 5 | – | – | – | 0.031 | 0.082 | – | – | 0.017 | 0.014 |
| 6 | – | $2.5\times10^{-3}$ | 0.05 | $9.63\times10^{-3}$ | 0.026 | $8.2\times10^{-3}$ | $3.2\times10^{-3}$ | $5.4\times10^{-3}$ | 0.35 |
| 7 | – | – | – | – | $6.0\times10^{-3}$ | – | – | $1.3\times10^{-3}$ | 7 |
| 8 | – | – | $5\times10^{-5}$ | – | $1.0\times10^{-3}$ | – | $8\times10^{-7}$ | $0.2\times10^{-3}$ | 92.6 |

$7^+$ ($^{184}$Pt) states we show only results from the DF model. The composition of the $8^-$ state cannot be predicted by the simple models presented; therefore, the $K$ distribution for this state was taken from calculations performed for $^{182}$Os [7], where the same $I^{\pi} = 8^-$, $K = 8$ isomeric state is observed. The authors of Ref. [7] claim that for other nuclei with $N = 106$ the results are very similar. We also used these results in the discussion of the $^{134}$Nd nucleus, where the $8^-$ isomeric state has an analogous structure (two quasineutron $\nu 7/2 \otimes \nu 9/2$ state).

As can be seen from Table V the Coriolis (rotational $K$-mixing) and DF models give quite different distributions of the $K$ components in the wave functions of the positive-parity states. To estimate the relative importance of the effects taken into account by the two models, we simply consider the products of the probabilities of the $K$ components in the wave function of the isomeric state and the state into which the isomer decays. The considered $K$ values take into account the experimental transition multipolarities discussed in this work and the $K$ selection rule.

Of course, such an analysis can yield only qualitative conclusions.

$^{134}$Nd, $8^- \to 6^+$, *874-keV E3 transition*. For this transition we also consider the $M2$ multipolarity, not excluded by the experimental data. First we discuss the DF model. In the case of the $E3$ branch the greatest probability products give two combinations, $(8^-, K = 7) \to (6^+, K = 4)$ and $(8^-, K = 5) \to (6^+, K = 2)$, with respective values of 8.4 and 0.54. For the $M2$ branch there are also two important combinations, $(8^-, K = 6) \to (6^+, K = 4)$ and $(8^-, K = 8) \to (6^+, K = 6)$, with respective values of 0.42 and 0.2. Within the Coriolis model and for the $E3$ branch one should consider two combinations, $(8^-, K = 8) \to (6^+, K = 5)$ and $(8^-, K = 7) \to (6^+, K = 4)$, with values of 2.9 and 0.54. For the $M2$ branch there are again

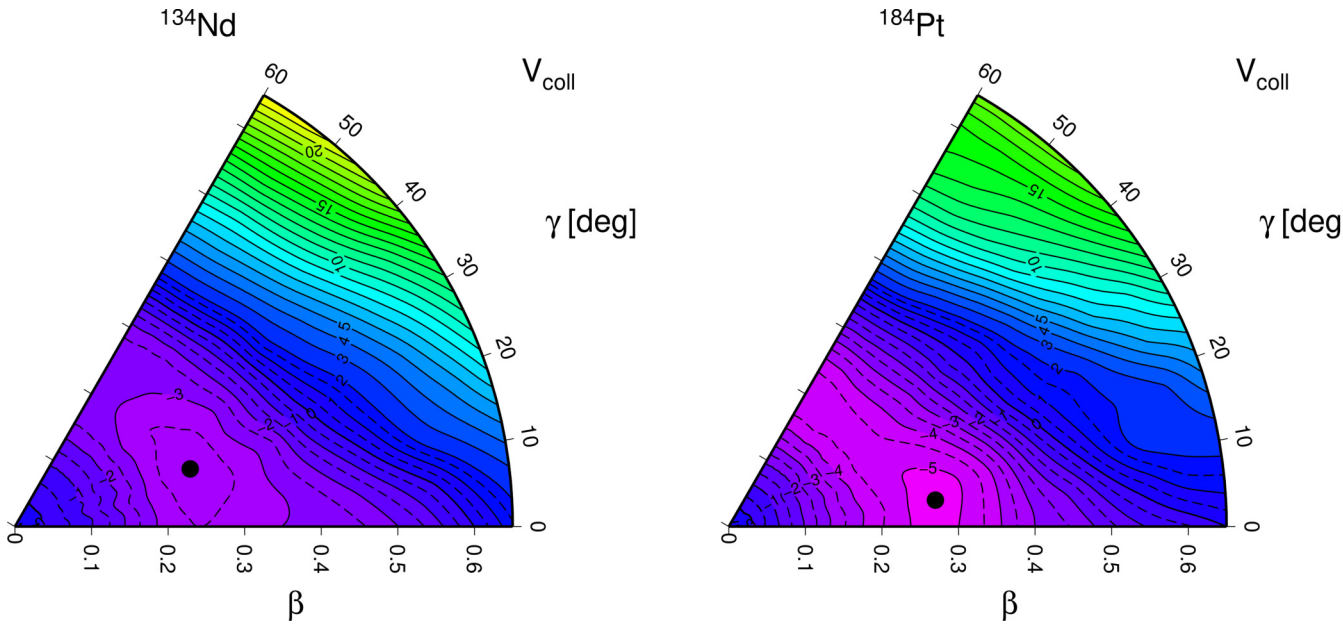


FIG. 11. Mean-field collective potential energy (relative to a spherical shape) for $^{134}$Nd and $^{184}$Pt (see text).

two combinations, $(8^-, K = 8) \rightarrow (6^+, K = 6)$ and $(8^-, K = 7) \rightarrow (6^+, K = 5)$, with values of 0.89 and 0.22.

$^{134}$Nd, $8^- \rightarrow 8^+$, *168-keV E*1 *transition*. In the DF model the best combination $(8^-, K = 7) \rightarrow (8^+, K = 6)$ gives a value of the product equal to 0.32, while other combinations can be neglected. In the Coriolis model there are again two relevant combinations, $(8^-, K = 8) \rightarrow (8^+, K = 7)$ and $(8^-, K = 7) \rightarrow (8^+, K = 6)$, with values of 0.56 and 0.18.

$^{184}$Pt, $8^- \rightarrow 8^+$, *610-keV E*1 *transition*. The DF model gives the biggest product for the combination $(8^-, K = 7) \rightarrow (8^+, K = 6)$ but with a value of only 0.023, while within the Coriolis model for the combination $(8^-, K = 8) \rightarrow (8^+, K = 7)$ the probability product is equal to 0.12.

The general qualitative conclusion is that both rotational $K$ mixing and triaxiality effects should be taken into account in explaining the reduction of the hindrance of the $K$-isomer decay. To get a quantitative interpretation of the experimental results, one needs a more complete theory for both the isomers and the states into which they decay.

## IV. SUMMARY

The decays of two $I^{\pi} = 8^-$, $K = 8$ isomeric states in $^{134}_{60}Nd_{74}$ and $^{184}_{78}Pt_{106}$ have been studied. The experiments were carried out in $e$-$\gamma$ and $\gamma$-$\gamma$ coincidence mode using electron spectrometers coupled to the EAGLE array. As a result of these measurements the internal conversion coefficients, multipolarities, and absolute transition probabilities were obtained.

In the case of $^{134}$Nd the internal conversion coefficient $[\alpha_K = 0.005(2)]$ for the $8^- \rightarrow 6^+$, 874-keV transition from the decay of the $8^-$ isomeric state was measured. The result implies a pure $E3$ or, in the limit of the experimental uncertainty, a mixed $E3/M2$ character. A previous suggestion [12] of an $M2$ multipolarity for this transition was based only on systematics. The very weak 596-keV $\gamma$ line accompanying the $8^-$ isomeric state decay to the $(5^+)$ state (a member of the $\gamma$ band) was observed in the present work for the first time. Its intensity is equal to 0.6(2)%, while the total intensity of all $\gamma$ transitions deexciting the $8^-$ isomeric state equals 100%; see Fig. 1 and Table I. The presence of the 596-keV transition was postulated in Ref. [10] but not experimentally proved. In our experiment the half-life of the $8^-$ isomeric state was determined as 0.38(2) ms.

In the case of $^{184}$Pt the internal conversion coefficients, multipolarities, and mixing parameters were determined for 119-keV transition. For the weak transitions, namely the 424- and 488-keV $\gamma$ lines, only upper limits for the ICCs were obtained. Nevertheless, these data allowed us to obtain information about the transition multipolarities. In all the cases studied (see Tables II and III) the results do not contradict the spins and parities proposed in Ref. [13], but for the 424- and 488-keV transitions other, additional solutions shown in Table III are possible. The half-life of the $8^-$ isomeric state measured in our experiment equals 0.86(10) ms.

Schematic theoretical models (VMI plus two band mixing and the Davydov-Filippov model) were applied to investigate the role of the Coriolis interaction (rotational $K$ mixing) and triaxiality in the weakening of the $K$ forbiddenness in the decay of the considered isomeric states. An analysis utilizing the transition multipolarities determined in this work and those taken from the literature shows that, besides the widely discussed rotational $K$ mixing, nonaxiality of the nucleus should also be taken into account in the theoretical description of the $K$-isomer decay.

## ACKNOWLEDGMENTS

We are grateful to Alison Bruce for very helpful discussions, in particular of the Coriolis $K$-mixing mechanism. The authors wish to thank the staff of the Heavy Ion Laboratory of the University of Warsaw for providing excellent beam conditions and for their support at each stage of this work. The possibility to use the Phase I ACS Ge detectors loaned by the GAMMAPOOL is gratefully acknowledged. This project was supported by grants from the Polish National Science Centre (Grants No. 2011/03/B/ST2/02660 and No. 2013/10/M/ST2/00427).

[1] A. K. Jain, B. Maheshwari, S. Garg, M. Patial, and B. Singh, Nucl. Data Sheets **128**, 1 (2015).

[2] P. M. Walker, G. Sletten, N. L. Gjorup, M. A. Bentley, J. Borggreen, B. Fabricius, A. Holm, D. Howe, J. Pedersen, J. W. Roberts, and J. F. Sharpey-Schafer, Phys. Rev. Lett. **65**, 416 (1990).

[3] A. M. Bruce, A. P. Byrne, G. D. Dracoulis, W. Gelletly, T. Kibèdi, F. G. Kondev, C. S. Purry, P. H. Regan, C. Thwaites, and P. M. Walker, Phys. Rev. C **55**, 620 (1997).

[4] P. M. Walker and G. D. Dracoulis, Nature (London) **399**, 35 (1999).

[5] T. Morek, J. Srebrny, C. Droste, M. Kowalczyk, T. Rzaca-Urban, K. Starosta, W. Urban, R. Kaczarowski, E. Ruchowska, M. Kisieliński, A. Kordyasz, J. Kownacki, M. Palacz, E. Wesołowski, W. Gast, R. M. Lieder, P. Bednarczyk, W. Męczyński, and J. Styczeń, Phys. Rev. C **63**, 034302 (2001).

[6] A. P. Robinson, T. L. Khoo, I. Ahmad, S. K. Tandel, F. G. Kondev, T. Nakatsukasa, D. Seweryniak, M. Asai, B. B. Back, M. P. Carpenter, P. Chowdhury, C. N. Davids, S. Eeckhaudt, J. P. Greene, P. T. Greenlees, S. Gros, A. Heinz, R.-D. Herzberg, R. V. F. Janssens, G. D. Jones, T. Lauritsen, C. J. Lister, D. Peterson, J. Qian, U. S. Tandel, X. Wang, and S. Zhu, Phys. Rev. C **78**, 034308 (2008).

[7] G. D. Dracoulis, G. J. Lane, F. G. Kondev, H. Watanabe, D. Seweryniak, S. Zhu, M. P. Carpenter, C. J. Chiara, R. V. F. Janssens, T. Lauritsen, C. J. Lister, E. A. McCutchan, and I. Stefanescu, Phys. Rev. C **79**, 061303 (2009).

[8] F. G. Kondev, G. D. Dracoulis, and T. Kibedi, At. Data Nucl. Data Tables **103–104**, 50 (2015).

[9] J. Perkowski, J. Andrzejewski, J. Srebrny, A. M. Bruce, C. Droste, E. Grodner, M. Kisieliński, A. Korman, M. Kowalczyk, J. Kownacki, A. Krol, J. Marganiec, J. Mierzejewski, T. Morek, K. Sobczak, W. H. Trzaska, and M. Zielińska, Eur. Phys. J. A **42**, 379 (2009).

[10] T. Morek and the Warsaw OSIRIS II Collaboration, Acta Phys. Pol. B **32**, 2537 (2001).

[11] E. A. McCutchan, R. F. Casten, V. Werner, R. J. Casperson, A. Heinz, J. Qian, B. Shoraka, J. R. Terry, E. Williams, and R. Winkler, Phys. Rev. C **87**, 057306 (2013).
[12] A. A. Sonzogni, Nucl. Data Sheets **103**, 1 (2004).
[13] C. M. Baglin, Nucl. Data Sheets **111**, 275 (2010).
[14] J. Burde, R. M. Diamond, and F. S. Stephens, Nucl. Phys. **85**, 481 (1966).
[15] J. Perkowski, J. Andrzejewski, T. Abraham, W. Czarnacki, C. Droste, E. Grodner, L. Janiak, M. Kisieliński, M. Kowalczyk, J. Kownacki, J. Mierzejewski, A. Korman, J. Samorajczyk, J. Srebrny, A. Stolarz, and M. Zielińska, Acta Phys. Pol. B **43**, 273 (2012).
[16] A. S. Davydov and G. F. Filippov, Nucl. Phys. **8**, 237 (1958).
[17] A. Bohr and B. R. Mottelson, *Nuclear Structure* (World Scientific, London, UK, 1999).
[18] J. Mierzejewski, J. Srebrny, H. Mierzejewski, J. Andrzejewski, W. Czarnacki, C. Droste, E. Grodner, A. Jakubowski, M. Kisieliński, M. Komorowska, A. Kordyasz, M. Kowalczyk, J. Kownacki, A. Pasternak, J. Perkowski, A. Stolarz, M. Zielińska, and R. Anczkiewicz, Nucl. Instrum. Methods Phys. Res., Sect. A **659**, 84 (2011).
[19] J. Andrzejewski, A. Krol, J. Perkowski, K. Sobczak, R. Wojtkiewicz, M. Kisieliński, M. Kowalczyk, J. Kownacki, and A. Korman, Nucl. Instrum. Methods Phys. Res., Sect. A **585**, 155 (2008).
[20] J. Perkowski, J. Andrzejewski, L. Janiak, J. Samorajczyk, T. Abraham, C. Droste, E. Grodner, K. Hadyńska-Klek, M. Kisieliński, M. Komorowska, M. Kowalczyk, J. Kownacki, J. Mierzejewski, P. Napiorkowski, A. Korman, J. Srebrny, A. Stolarz, and M. Zielińska, Rev. Sci. Instrum. **85**, 043303 (2014).
[21] D. C. Radford, Nucl. Instrum. Methods Phys. Res., Sect. A **361**, 297 (1995).
[22] J. Samorajczyk, J. Andrzejewski, L. Janiak, J. Perkowski, J. Skubalski, and A. Stolarz, Acta Phys. Pol. B **43**, 325 (2012).
[23] T. Kibedi, T. W. Burrows, M. B. Trzhaskovskaya, P. M. Davidson, C. W. Nestor, and C. W. Nestor, Nucl. Instrum. Methods Phys. Res., Sect. A **589**, 202 (2008).
[24] T. Venkova, T. Morek, G. V. Marti, H. Schnare, A. Kramer-Flecken, W. Gast, A. Georgiev, G. Hebbinghaus, R. M. Lieder, G. Sletten, K. M. Spohr, K. H. Maier, and W. Urban, Z. Phys. A **344**, 417 (1993).
[25] G. D. Dracoulis, P. M. Walker, and F. G. Kondev, Rep. Prog. Phys. **79**, 076301 (2016).
[26] B. Crowell, P. Chowdhury, D. J. Blumenthal, S. J. Freeman, C. J. Lister, M. P. Carpenter, R. G. Henry, R. V. F. Janssens, T. L. Khoo, T. Lauritsen, Y. Liang, F. Soramel, and I. G. Bearden, Phys. Rev. C **53**, 1173 (1996).
[27] S. Nilsson and I. Ragnarsson, *Shapes and Shells in Nuclear Structure* (Cambridge University Press, Cambridge, UK, 1995).
[28] M. A. J. Mariscotti, G. Scharff-Goldhaber, and B. Buck, Phys. Rev. **178**, 1864 (1969).
[29] L. Próchniak and S. Rohoziński, J. Phys. (London) G **36**, 123101 (2009).
[30] K. Wrzosek-Lipska, L. Próchniak, M. Zielińska, J. Srebrny, K. Hadyńska-Klek, J. Iwanicki, M. Kisieliński, M. Kowalczyk, P. J. Napiorkowski, D. Pietak, and T. Czosnyka, Phys. Rev. C **86**, 064305 (2012).
[31] P. J. Napiorkowski, DF code, accessible online at http://www.slcj.uw.edu.pl/~pjn/DF/DF.htm.